

# A Comparison of the performance and wear characteristics of high-speed steel circular saw blades machining Nimonic PK31,\* AISI O1 Tool Steel, Inconel 600L,\* and AISI 1018 Carbon Steel

S. R. BRADBURY

*Department of Mechanical Engineering, University of Sheffield, Sheffield UK*

D. B. LEWIS

*Materials Research Institute, Sheffield Hallam University, Sheffield UK*

High-speed steel circular saw blades are widely used in industry for a variety of cut-off operations that require a combination of high-dimensional accuracy and a good-quality surface finish. The authors have been involved in an extensive programme of work to evaluate the effectiveness of applying advanced surface engineering treatments to enhance the performance and life characteristics of this form of tool. The work included optimizing cutting conditions with respect to tool performance when machining different workpiece materials, characterizing the wear mechanisms developed throughout tool life, and evaluating of the effect of different substrate surface preparations and advanced surface engineering treatments on the performance and wear characteristics of the tool.

One interesting feature to arise from the work that has not been reported elsewhere has been the notable variation in performance and wear characteristics of nominally identical tools machining materials with similar hardness. The current paper compares the performance and wear characteristics of high-speed steel circular saw blades machining a tool steel and a nimonic nickel-based alloy (340–390 H<sub>v</sub>). These are termed “difficult to cut” materials because of their poor machinability. A comparison is also made of the performance and wear characteristics of an Inconel nickel-based alloy and a low-carbon steel (120–150 H<sub>v</sub>), both of which exhibit good machining characteristics. Differences identified between the resulting wear mechanisms emphasize the difficulties inherent in developing a universal tooth geometry and advanced surface engineering coating system that would be effective for all machining applications. © 2000 Kluwer Academic Publishers

## 1. Introduction

Through improved frictional, thermal, and wear-resistance characteristics, advanced surface engineering treatments have been successfully applied to indexable inserts [1] and high-speed steel drills [2], enabling them to operate at higher feeds and faster cutting speeds, without coolant and over a wider range of applications. Comparable benefits have yet to be fully realized when applying the same technologies to multipoint cutting tools such as saws, milling cutters, and broaches. Factors that have adversely affected the application of advanced surface engineering coatings to this form of tool include

1. quality and consistency of manufacture [3]
2. size limitations/access restrictions within the coating chamber

Another significant factor is the manner in which single-point and multipoint cutting tools wear. Single-point tools, such as indexable inserts, are relatively simple in their metal removal characteristics, and to a great extent the resulting wear mechanisms are both consistent and predictable. The chip formation and wear mechanisms associated with multipoint cutting tools are far more complex, inconsistent, and unpredictable [4].

The current paper compares the performance and wear mechanisms associated with high-speed steel circular saw blades cutting two materials with characteristic poor machinability, namely AISI O1 tool steel and Nimonic PK31 nickel-based alloy. AISI O1 is a standard abrasion-resistant tool steel commonly used for hammers, chisels, and soon whereas Nimonic PK31 is highly resistant to creep, fatigue, oxidation, and thermal shock and is used for applications that require high

\*Registered trademark of the Inco family of companies

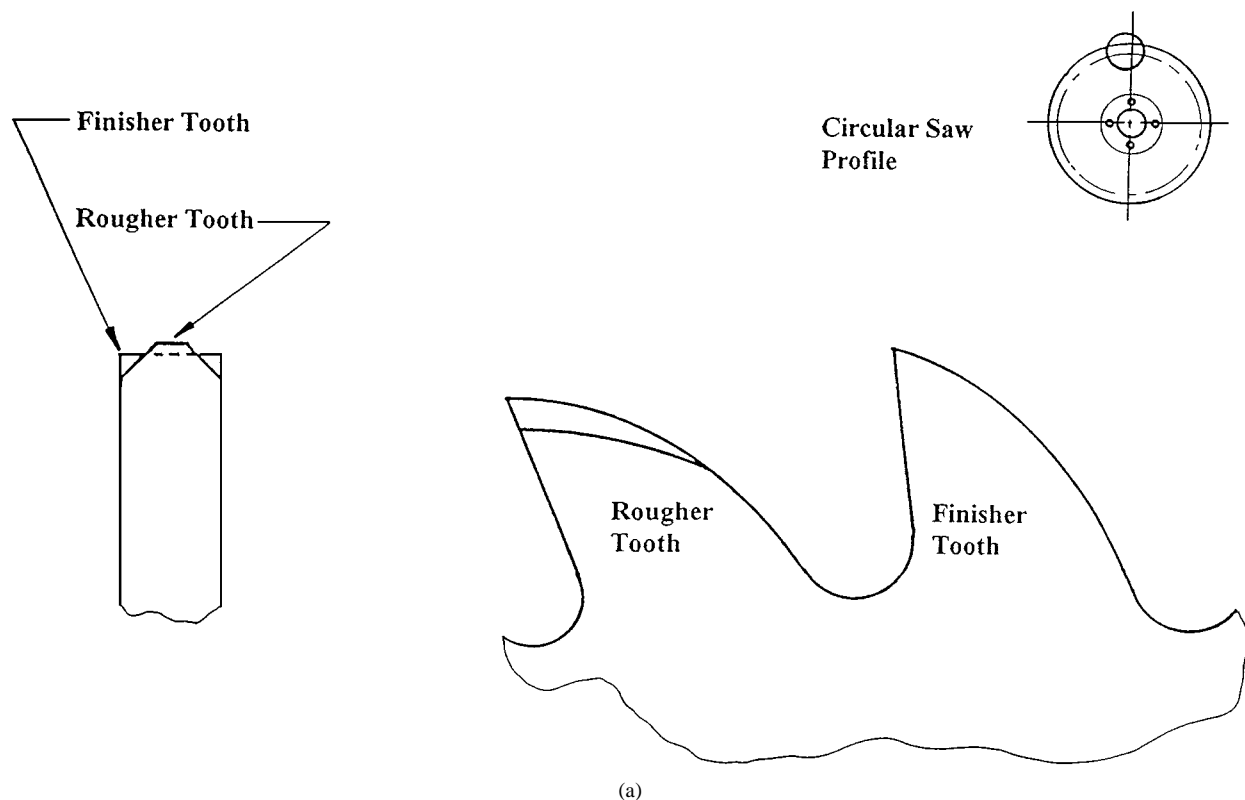


Figure 1 Circular saw geometry.

strength and durability under severe thermal conditions, most notably in jet engines. These materials have a similar hardness: 340–390  $H_v$ .

A second comparison of the performance and wear characteristics is made for the same tool cutting two materials with a characteristic good machinability, namely Inconel 600L nickel-based alloy and AISI 1018 carbon steel in an annealed condition. Inconel 600L nickel-based alloy exhibits high resistance to oxidation and corrosion resistance at high temperatures and is used for components that require a long service life while operating under thermally hostile conditions. AISI 1018 is a standard grade of carbon steel used for lightly stressed parts produced by cold-forming processes. Both materials have a similar hardness: 120–150  $H_v$ .

Analysis of blade performance highlights the relatively poor machinability of the nimonic nickel-based alloy compared with the other workpiece materials; comparison of the resulting wear mechanisms emphasizes the difficulty in developing a universally applicable tool geometry and surface engineering coating system.

## 2. Experimental and evaluation techniques

Circular saw blades are used for industrial cut-off operations that require a relatively high degree of dimensional accuracy. The product is manufactured to a higher specification than either band saw or hacksaw blades are, thus giving greater potential for success in terms of enhanced performance, tool life, and range of application when applying advanced surface engineering coatings.

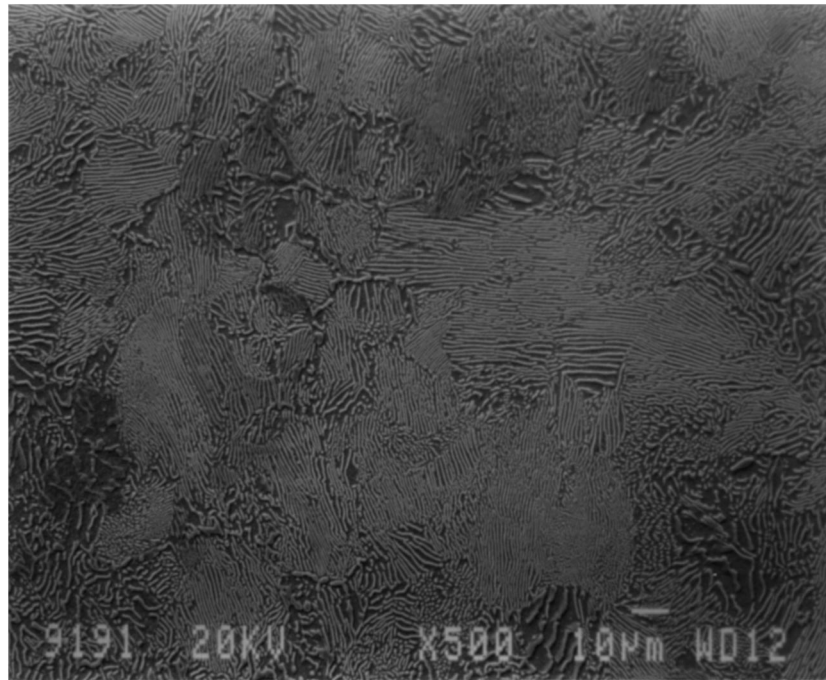
In the current work, M2 high-speed steel circular saw blades, 250 mm in diameter, 2.5 mm in thickness, with 160 teeth, were used to machine 20-mm square workpiece sections. The teeth of the blades were of the Heller profile, ground to the alternate rougher and finisher tooth configuration shown in Fig. 1.

Techniques have been developed to evaluate the optimum performance and the performance throughout life of a blade by testing either segments that contain a representative rougher and finisher tooth or full blades. Full details and verification of the techniques are published elsewhere [5]. For the current test programme, blade segments were used.

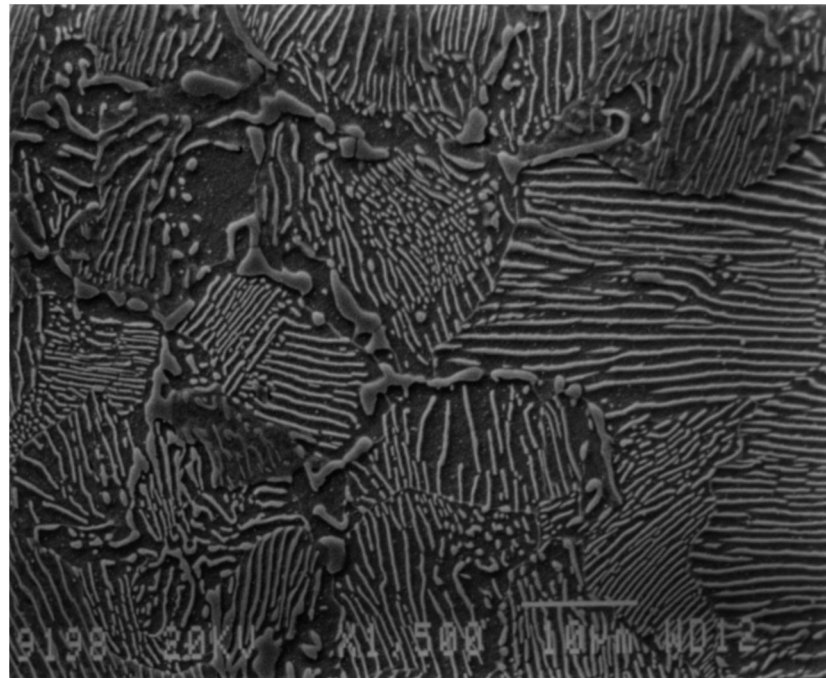
TABLE I Workpiece material composition (%) and hardness ( $H_v$ ).

Material	C	Ni	Cr	Al	Ti	Co	Mo	Nb	$H_v$
AISI O1 Tool Steel	1.0	—	0.5	—	—	—	—	—	389
Nimonic PK31	—	53.0	20.0	0.4	2.4	14.0	4.5	5.0	340
Inconel 600L	—	76.0	15.5	—	0.3	—	—	—	146
AISI 1018 Steel	0.18	0.19	0.195	—	—	—	—	—	127

(AISI 1018 also contains Mn, 0.78%; Si, 0.21%; S, 0.022; and P, 0.022)



(a)



(b)

Figure 2 Microstructure of O1 tool steel; (a)  $\times 500$ , (b)  $\times 1500$ .

### 3. Workpiece material analysis

The composition and hardness of the workpiece materials used in the current investigation are given in Table I.

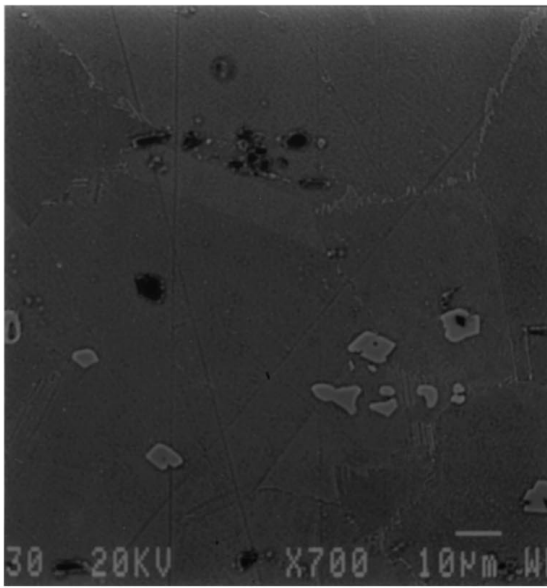
#### 3.1. AISI O1 tool steel

Components manufactured from this material are usually heat treated after machining, so they are not machined to size at this stage because some distortion is likely. When machined, AISI O1 is an abrasion-resistant material that tends to work harden and produce tough chips that are difficult to break. The micro-

graphs in Fig. 2 show the material to have a pearlitic microstructure.

#### 3.2. Nimonic PK31 nickel-based alloy

The micrograph in Fig. 3a identifies titanium nitride (dark) and niobium carbides (light) distributed throughout the microstructure of the material. This is confirmed by the X-ray distribution maps shown in Fig. 3b and c, respectively. At higher magnification, the presence of gamma prime within the matrix and carbide precipitation ( $M_{23}C_6$ ) along grain boundaries has also been



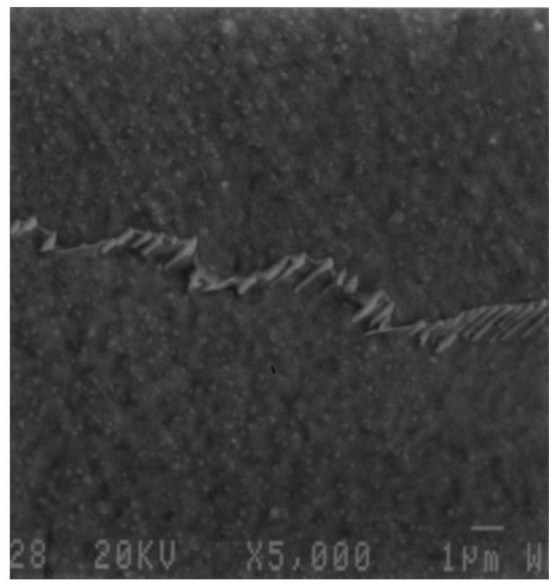
(a)



(b)

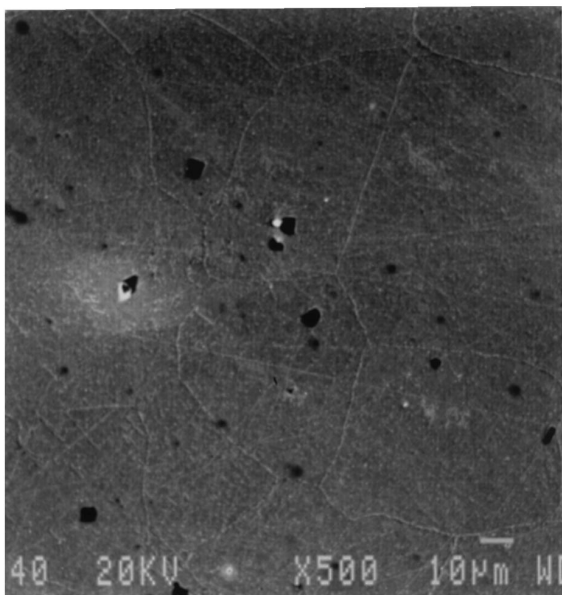


(c)

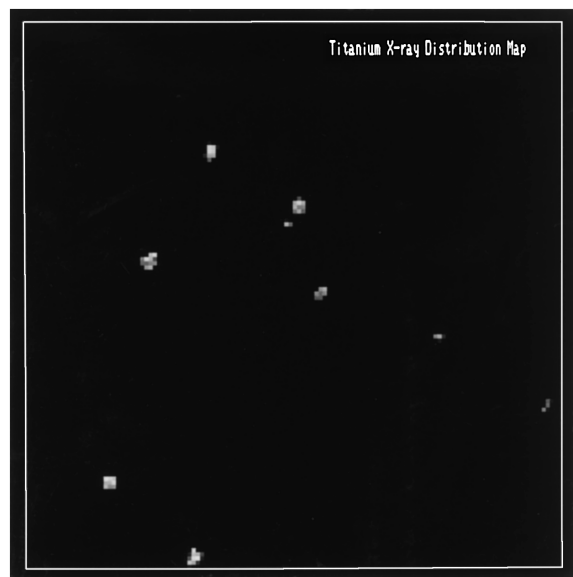


(d)

Figure 3 Microstructure of Nimonic PK31 nickel-based alloy (a)  $\times 700$ , (d)  $\times 5000$ ; (b) Ti; and (c) Nb X-ray distribution map  $\times 700$ .



(a)



(b)

Figure 4 Microstructure of Inconel 600L nickel-based alloy, (a)  $\times 500$ ; (b) Ti X-ray distribution map  $\times 700$ .

identified, Fig. 3d. The presence of these hard particles promotes abrasive wear if conditions allow; however, work hardening and adhesive wear predominate when this material is machined.

### 3.3. Inconel 600L nickel-based alloy

The micrograph shown in Fig. 4a shows particles of titanium nitride dispersed throughout the microstructure. This is confirmed by the X-ray distribution map for titanium shown in Fig. 4b. The presence of the titanium nitride particles promotes abrasive wear under sliding conditions along the tool and workpiece interface.

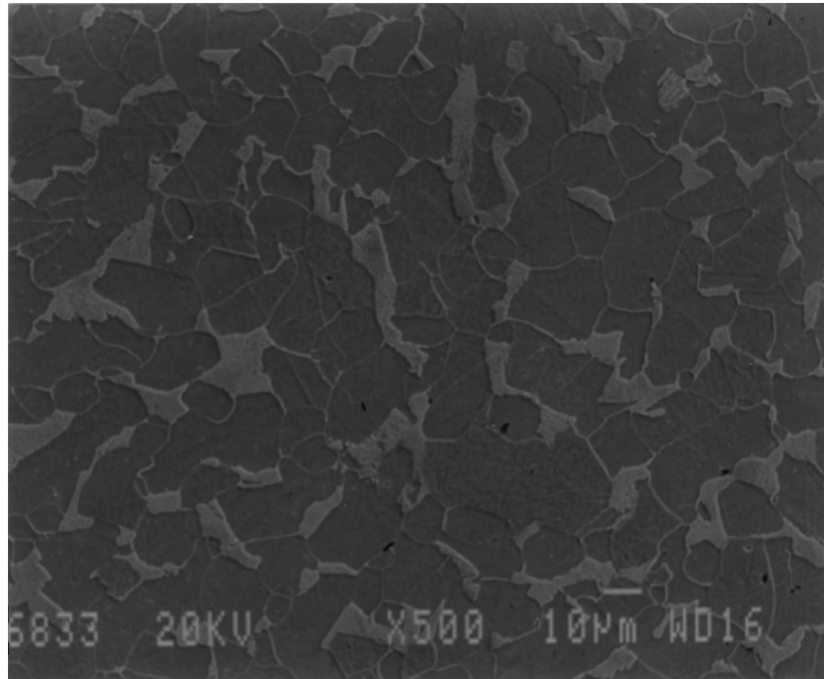
### 3.4. AISI 1018 carbon steel

The micrographs in Fig. 5 show predominantly a ferrite microstructure with small areas of pearlite.

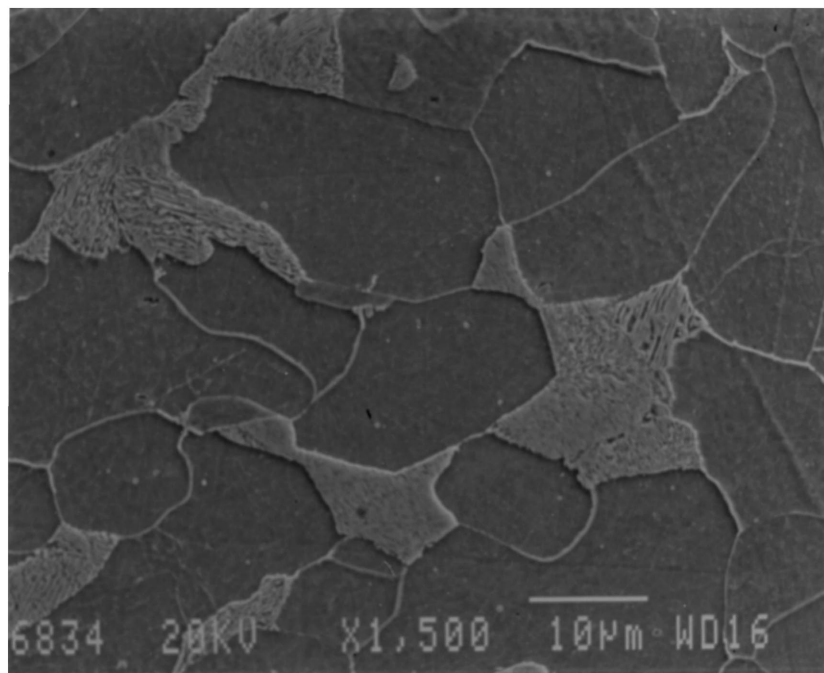
## 4. Experimental results and discussion

### 4.1. Cutting tests

The tools were tested to determine the optimum cutting conditions for machining each material and to monitor tool performance throughout its useful life when operating under optimized cutting conditions. In both cases the cutting force was measured using a three-force dynamometer. The cutting force was used to evaluate the



(a)



(b)

Figure 5 Microstructure of AISI 1018 carbon steel; (a)  $\times 500$ , (b)  $\times 1500$ .

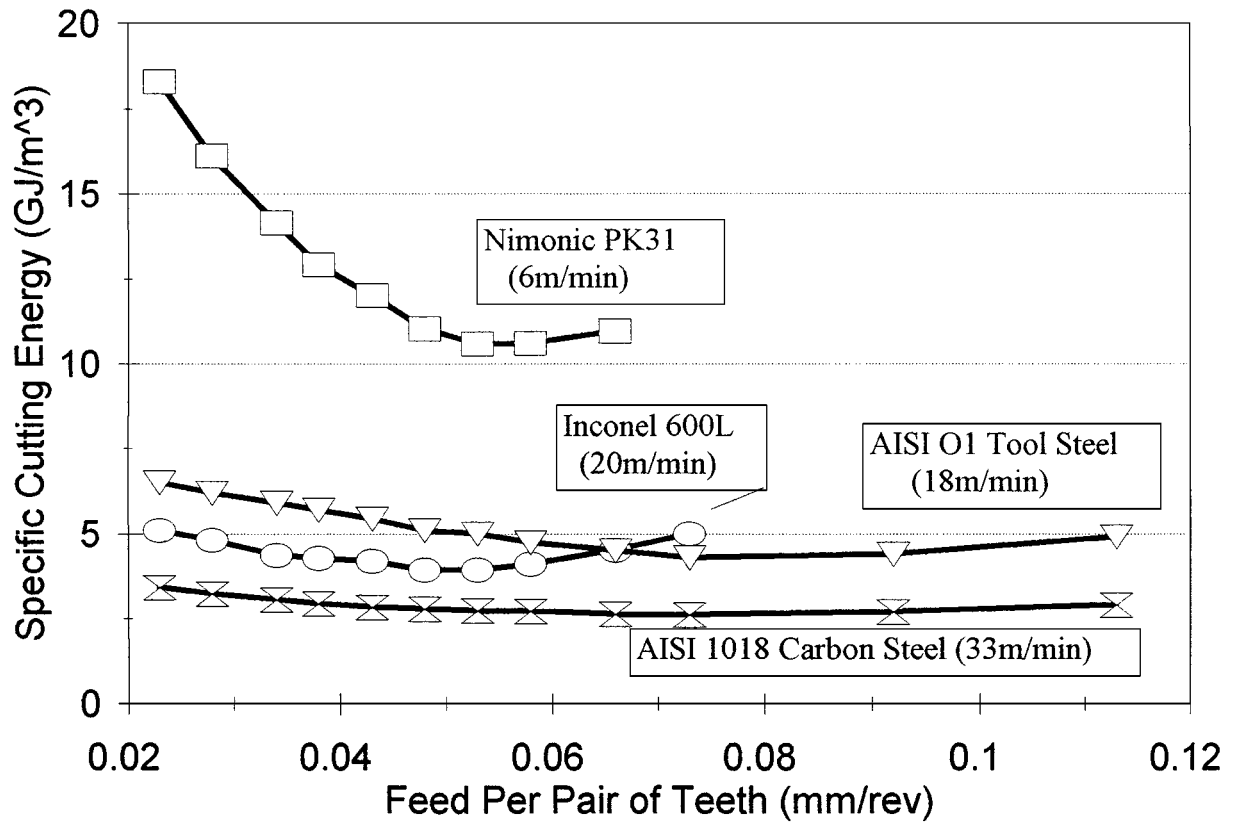


Figure 6 Optimized performance curves.

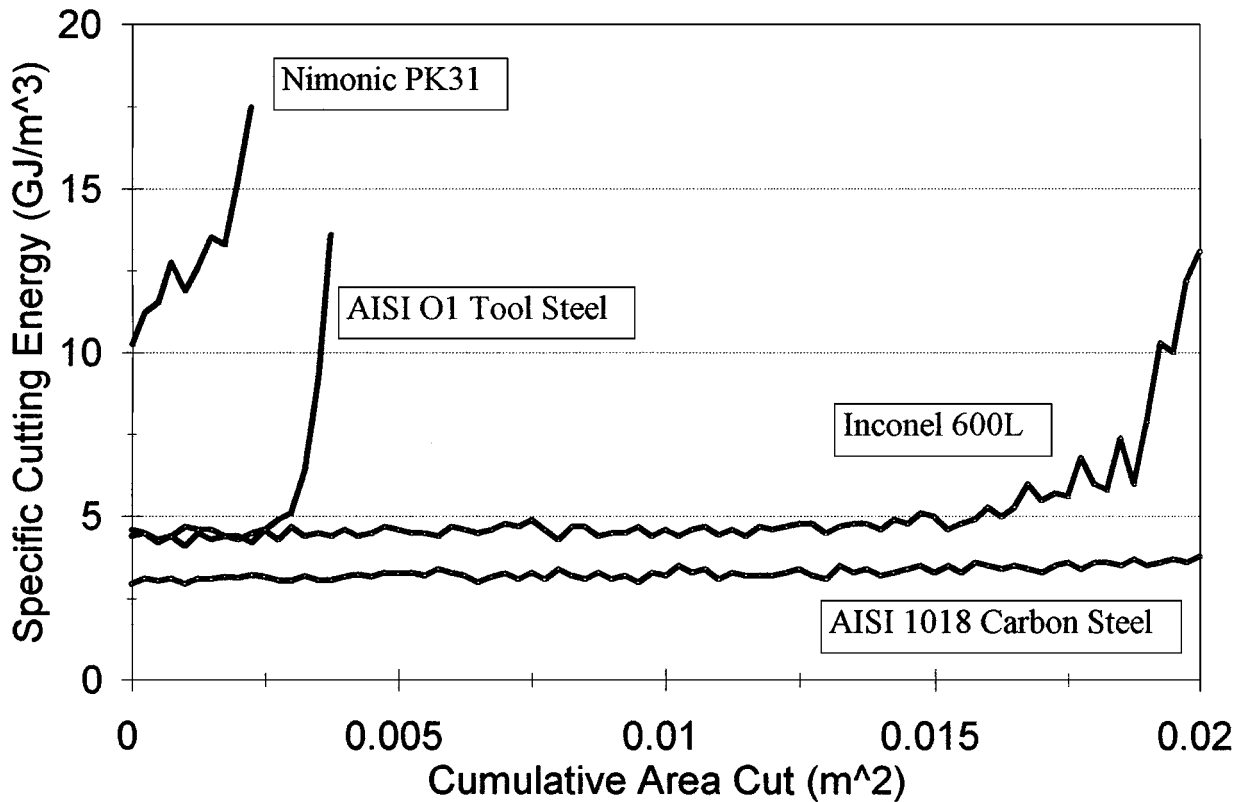


Figure 7 Performance throughout tool life.

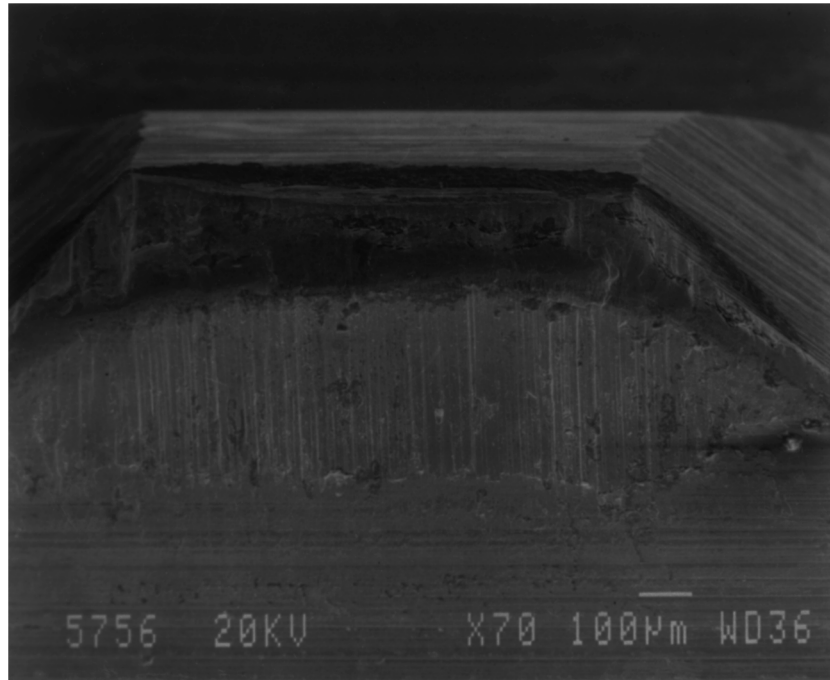
specific cutting energy ( $E_{sp}$ ). This parameter can be defined as a measure of the energy required to remove a specific volume of workpiece material (units:  $J/m^3$ ) [5] and has been widely used to evaluate cutting tool performance throughout tool life.

Blade segments were tested at a range of cutting speeds. At each cutting speed the feed rate was in-

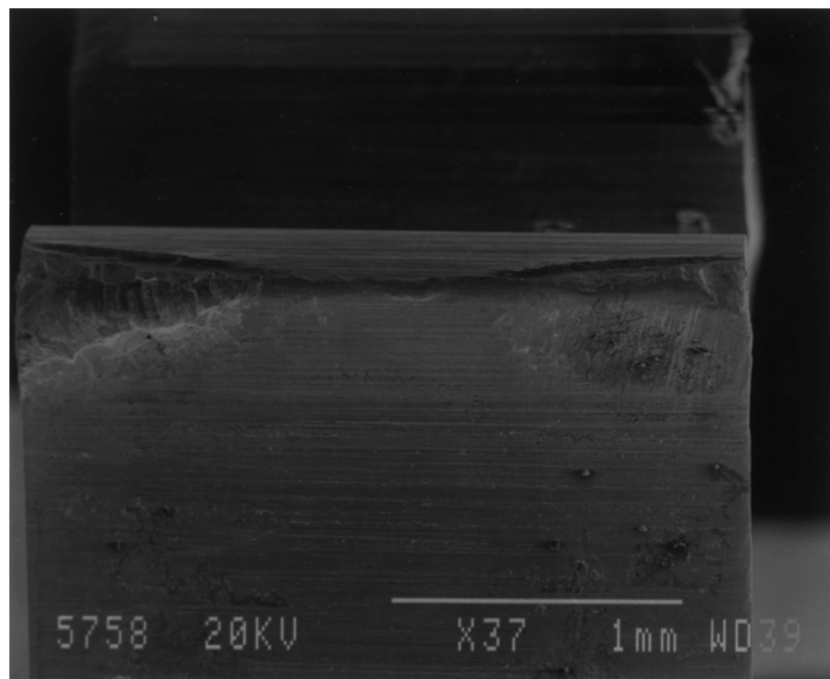
creased incrementally and the  $E_{sp}$  evaluated at each setting. As the feed rate increased the  $E_{sp}$  initially reduced in value until the effects of gullet congestion caused it to increase again. The combination of cutting parameters at which the energy requirements were a minimum were determined using this method [6]. Curves relating to the materials are given in Fig. 6 with the optimized

TABLE II Optimized Cutting Conditions

Workpiece Material	Cutting speed (m/min)	Feed [per pair of teeth] ( $\mu\text{m}/\text{rev}$ )	Cutting fluid
AISI O1 Tool Steel	18	73	Rocol 240 (2% sol)
Nimonic PK31	6	56	Rocol 240 (2% sol)
Inconel 600L	20	52	Rocol 240 (2% sol)
AISI 1018 Steel	33	72	Rocol 240 (2% sol)



(a)



(b)

Figure 8 Cutting edge topography of a (a) rougher and (b) finisher tooth: AISI O1 tool steel cutting tests.

cutting conditions listed in Table II. It should be noted that the optimum feed rates were found to be lower for the nickel-based alloys (0.05–0.055 mm/rev) when compared with the steels (0.07–0.075 mm/rev). This

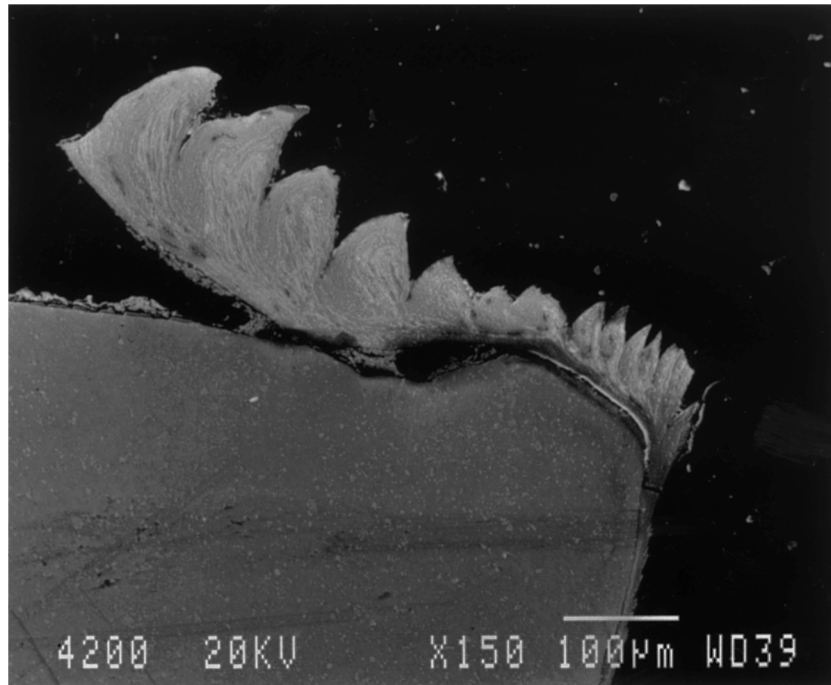
can be attributed to a high work-hardening rate that is associated with the machining of nickel-based alloys [7]. The performance throughout life of blade segments machining each material was then determined with the

machine tool set to the optimum cutting conditions, the results for which are shown in Fig. 7.

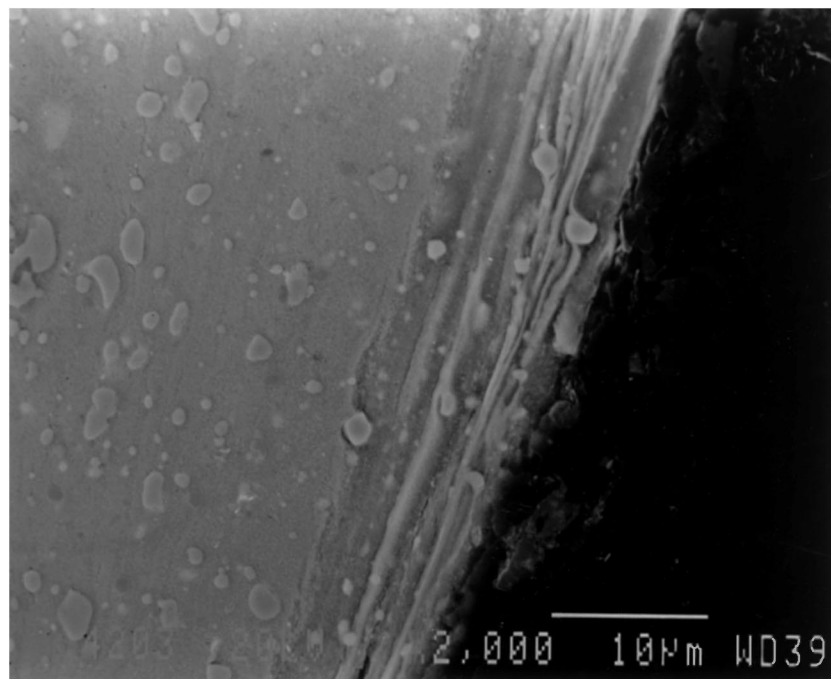
From Fig. 7 it is apparent that there is a large variation in energy requirements for machining the different materials. The minimum energy required to machine the nimonic alloy was approximately  $11 \text{ GJ m}^{-3}$ ; this compares with  $6.5 \text{ GJ m}^{-3}$  for the Inconel,  $5.5 \text{ GJ m}^{-3}$  for the tool steel, and  $4 \text{ GJ m}^{-3}$  for the carbon steel. The conversion of a large proportion of the energy into heat results in the rapid failure of the tools. This is in-

dicated by the curves in Fig. 7 that show a massive increase in gradient toward the end of the life of each tool.

The minimum energy required to machine the tool steel and the Inconel alloy were shown to be similar at  $4.5 \text{ GJ m}^{-3}$ . Tool life when machining these materials was shown to differ greatly with the segments that machined the Inconel alloy sectioning  $0.02 \text{ m}^2$  cumulative area cut compared with  $0.0035 \text{ m}^2$  cumulative area cut for those that had machined the tool steel. It



(a)



(b)

Figure 9 Microstructure of a finisher tooth (section 0.4 mm in from side face): AISI O1 tool steel cutting tests.



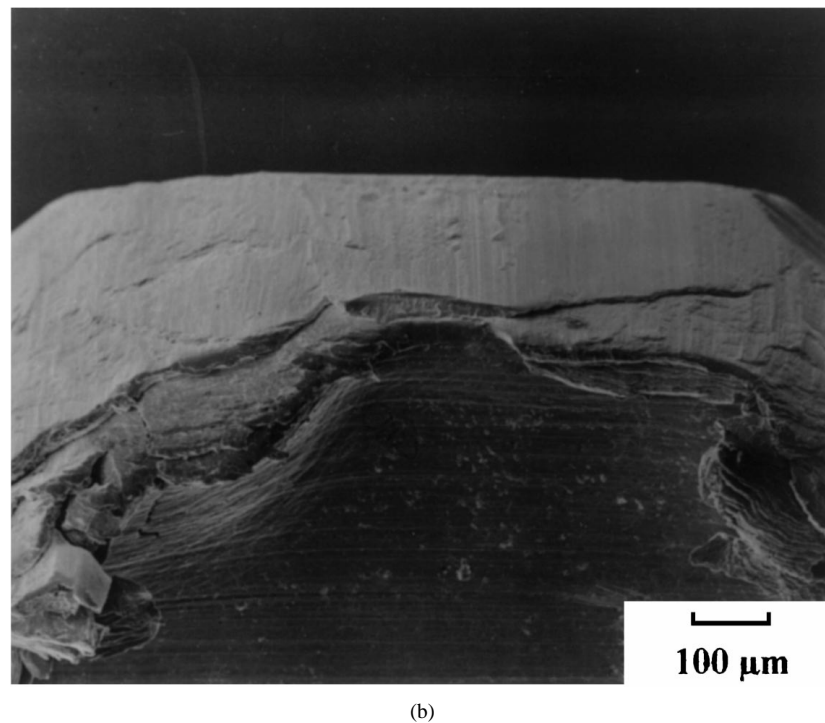
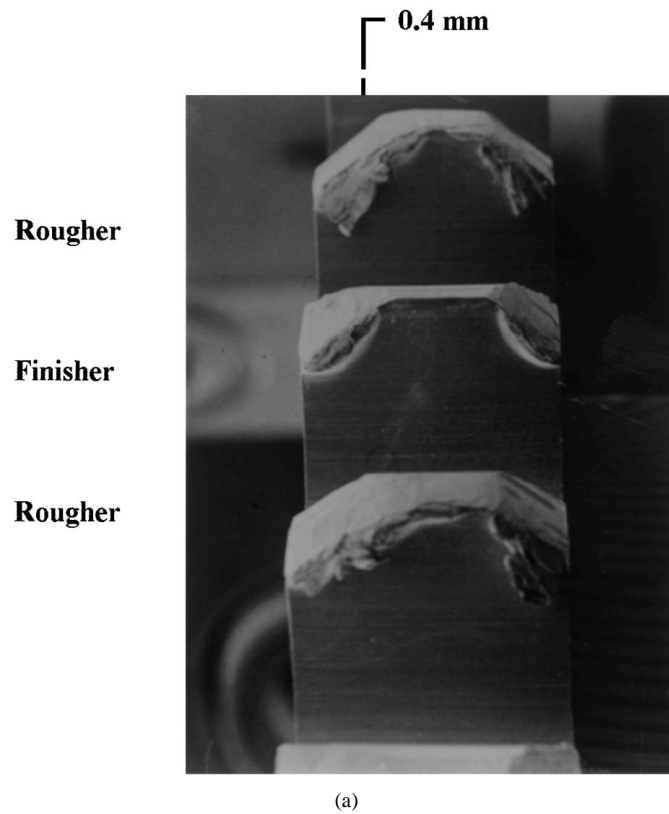


Figure 10 Wear mechanisms: Nimonic PK31 cutting tests.

is apparent that the materials must show different characteristics in terms the metal removal mechanism and the proportions of heat dissipated to chip, tool, workpiece, and coolant. This variation is investigated further by considering the resulting wear mechanisms. The energy required to machine the AISI 1018 carbon steel was low. This was reflected in the extensive life of the tool.

## 4.2. Examination of wear mechanisms

The wear mechanisms were investigated using scanning electron microscopy after  $0.0018 \text{ m}^2$  of each material had been cut.

### 4.2.1. AISI O1 tool steel

The micrographs in Fig. 8 show the cutting edge topography of a (a) rougher and (b) finisher tooth. The

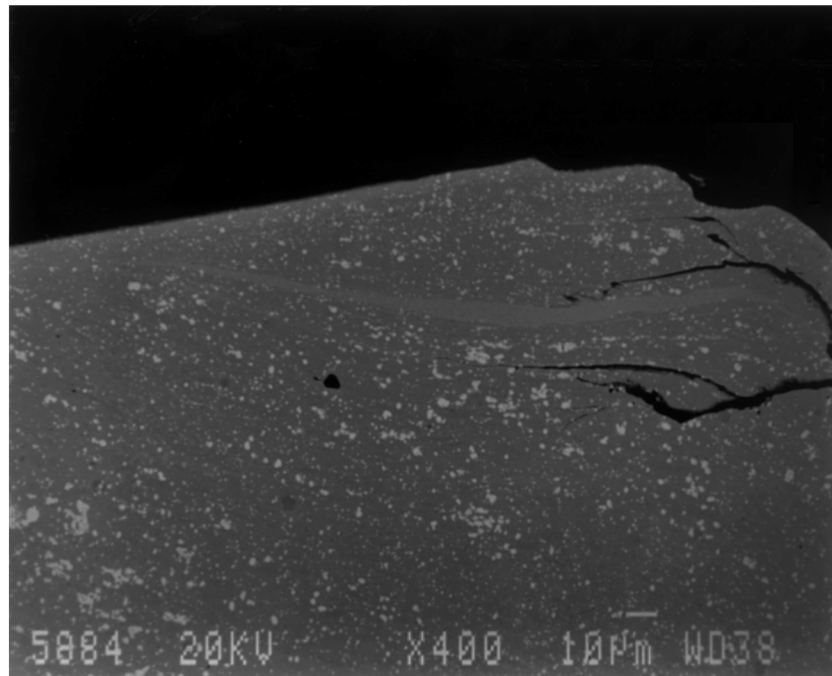
rougher tooth shows clear evidence of plastic deformation along the cutting edge and signs of abrasive wear on the rake face. The finisher tooth shows similar characteristics at the extremes of the cutting edge (the center of this tooth is masked by the profile of the rougher tooth and hence shows no significant wear). There appears to be no significant wear on the clearance face of either tooth.

The wear mechanisms were further investigated by examining the microstructure of the tool by taking metallographic sections normal to the cutting edge of the

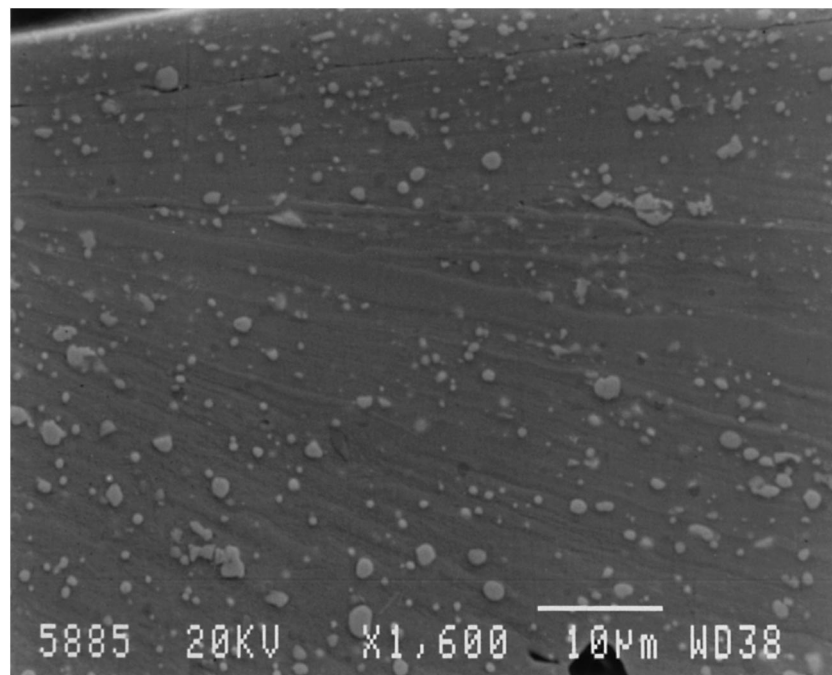
tooth. The micrograph in Fig. 9 shows the microstructure of a finisher teeth at a section 0.4 mm in from the side face. The micrograph shows plastic deformation of the cutting edge with evidence of cratering in the region of tool or chip separation.

#### 4.2.2. Nimonic PK31 nickel-based alloy

The teeth that had machined the nimonic alloy were severely worn. The micrograph in Fig. 10a shows loss of the Heller tooth profile, with the shape of both tooth

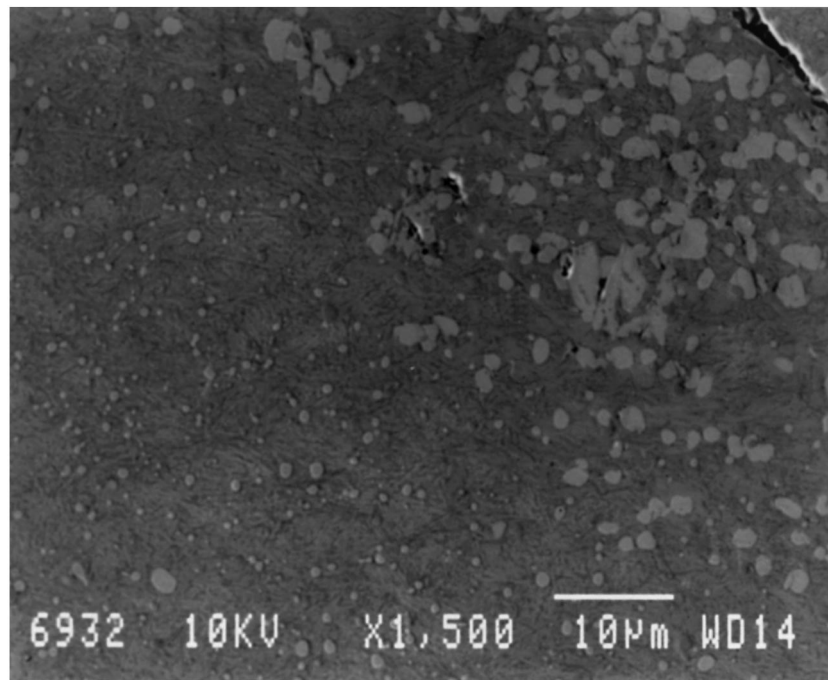


(a)



(b)

Figure 11 Microstructure of a finisher tooth (section 0.4 mm in from side face): Nimonic PK31 cutting tests.



(c)

Figure 11 (Continued).

forms appearing almost identical. Examination of the surface topography of a rougher tooth (Fig. 10b) shows massive plastic deformation along the cutting edge with a build-up of material extending down the rake face. Characteristic adhesive wear is evident along the clearance face. Similar wear mechanisms were identified on the finisher tooth.

The wear mechanisms were further investigated by considering the microstructure in metallographic sections prepared normal to the cutting edge of the tooth. The micrographs presented in Fig. 11 show the microstructure of a finisher teeth at a section 0.4 mm in from the side face following the nimonic cutting tests. This section was chosen because it passes directly through the region of most severe damage. It can be seen in Fig. 11a that the microstructure of the tool is characterized by cracks interspersed with bands of workpiece material that originate at the cutting edge and extend back along the clearance face. At higher magnification (Fig. 11b), extensive shearing of the tool material is apparent. There is also evidence of coalescence of the complex carbides, indicated by region A in Fig. 11c. Interpretation of the microstructure in accordance with Wright and Trent [8] indicated that in places the tool temperature had exceeded 900 °C.

#### 4.2.3. Inconel 600L nickel-based alloy

Preliminary examination of the teeth that had machined the Inconel alloy showed the accumulative wear to be an order of magnitude less than that identified with the blades that had machined the tool steel and the nimonic alloy. There was evidence of abrasive wear, however (Fig. 12a) and workpiece adhesion (Fig. 12b) along the cutting edge of a rougher tooth as characterized

by fine score marks and a flakey surface morphology, respectively.

#### 4.2.4. AISI 1018 steel

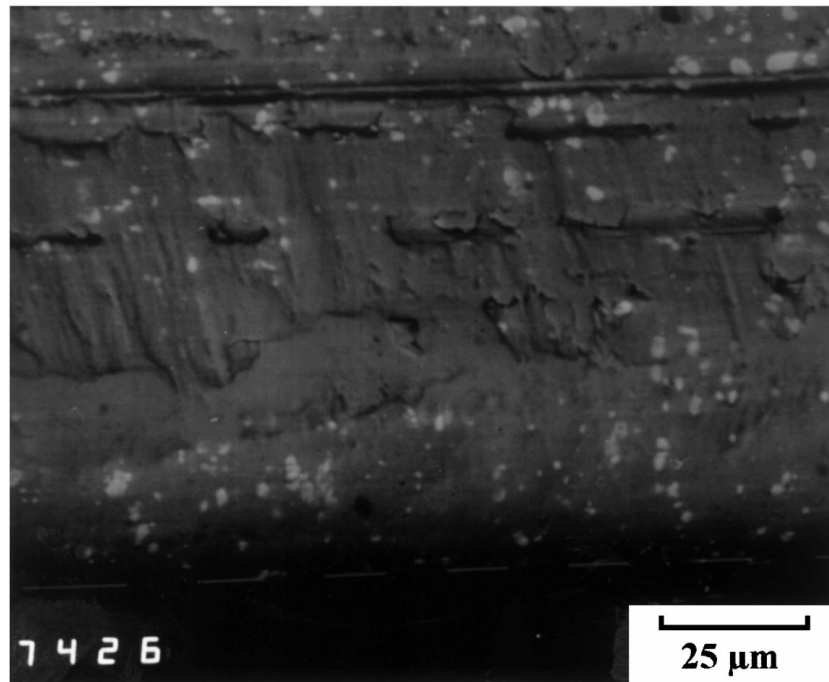
As with the tests machining the Inconel 600L the extent of wear was far less severe than exhibited by the teeth that had machined the tool steel and the nimonic alloy. Regions of wear are shown to be confined to the cutting edge (Fig. 13a), with both the rake and the clearance faces remaining unaffected.

Closer examination of the cutting edge (Fig. 13b) shows a “rounding off” and fine score marks projecting toward the clearance face. The score marks are a characteristic of abrasive wear under sliding conditions at the tool or chip interface.

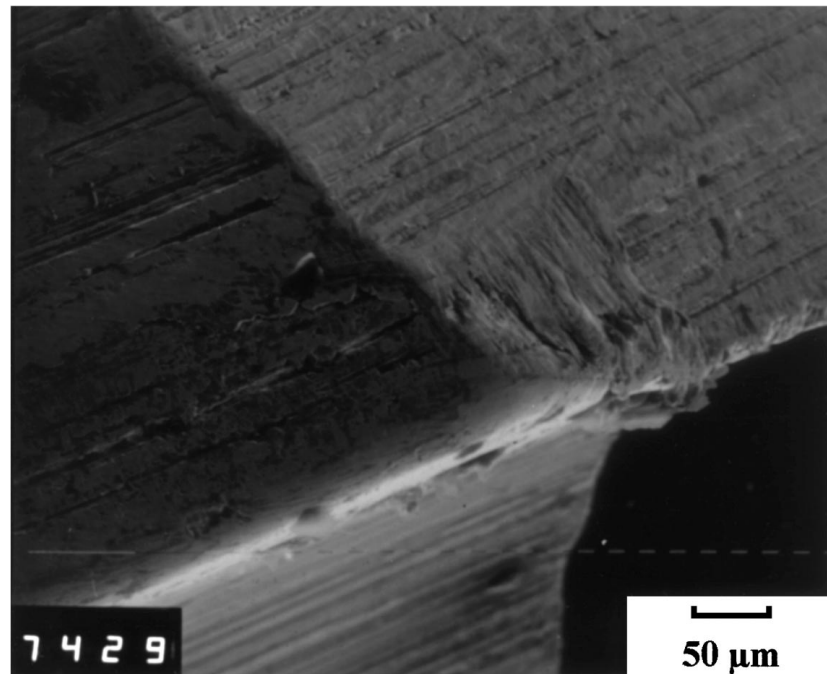
## 5. Conclusions

The investigation has identified fundamental differences in the mechanisms by which high-speed steel circular saw blades wear when machining a range of high- and low-machinability materials.

- Relatively poor machinability and rapid loss of performance have been shown to be a characteristic of the high-speed steel circular saw blades machining both the AISI O1 tool steel and the nimonic PK31 nickel-based alloy (see Fig. 4).
- The investigation has identified differences in the resulting wear mechanisms when machining these materials. On the teeth that machined the tool steel, the wear regime was confined to the region of the



(a)



(b)

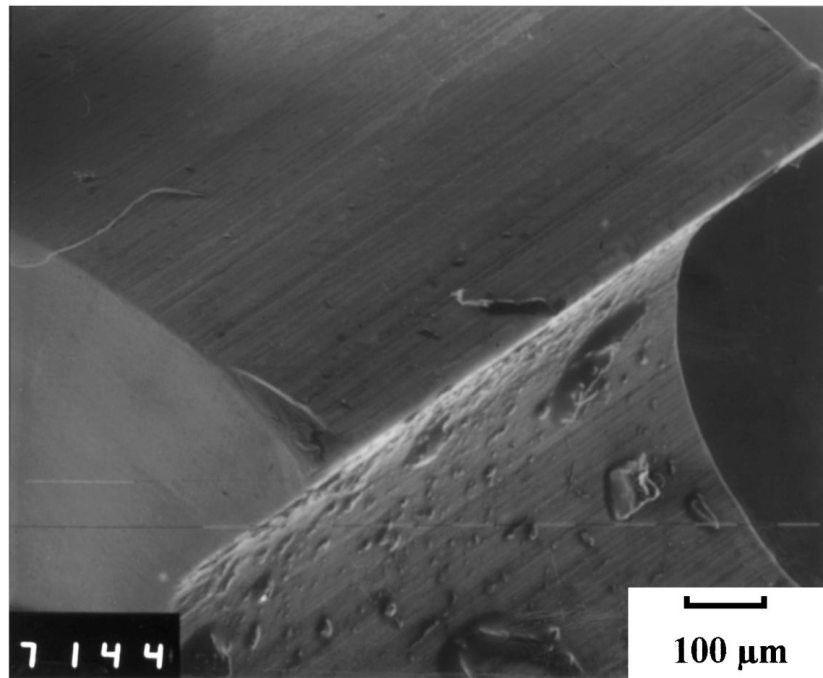
Figure 12 Wear mechanisms: Inconel 600L cutting tests.

cutting edge and rake face, with no evidence of wear along the clearance face. The wear modes were consistent with those described by Trent [9] for high speed steel tools machining austenitic stainless steel, where the tool or chip is in a state of seizure at the cutting edge and sliding contact down the rake face. The maximum temperature occurs at the point of tool or chip separation, which can lead to internal shear of the material, manifesting itself in the form of crater wear.

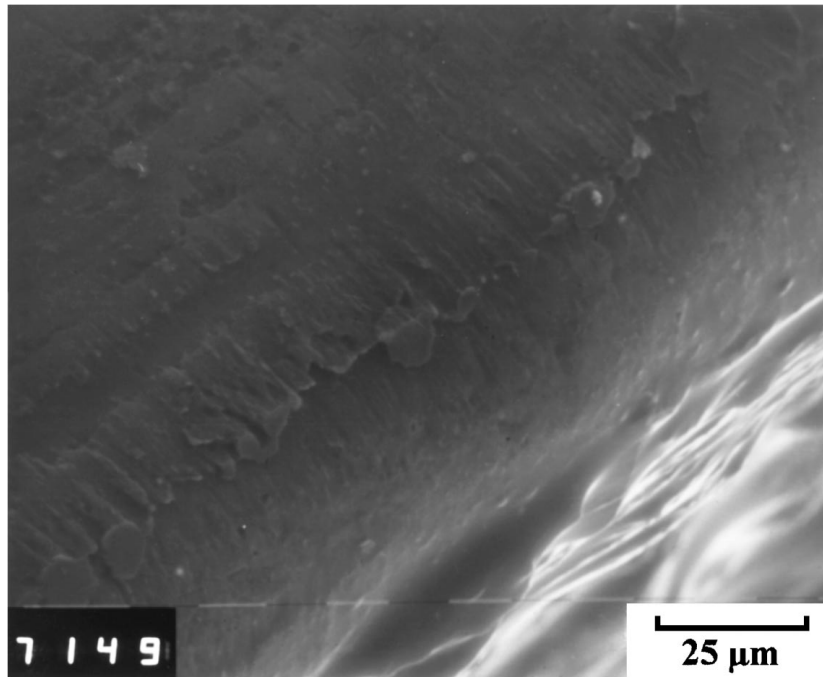
- Trent [9] states that when machining nickel-based

alloys the maximum temperature and resultant internal shear of the tool material occur at the cutting edge and also along the clearance face of badly worn tools. This is consistent with the wear mechanisms identified within the current investigation when machining the nimonic alloy. Temperatures in excess of 900 °C have been estimated within this region.

- The wear mechanisms identified on the teeth that machined the Inconel 600L and the AISI 1080 steel (Figs 12 and 13, respectively) were considerably



(a)



(b)

Figure 13 Wear mechanisms: AISI 1018 cutting tests.

less severe when compared with teeth that had machined a similar amount of the other two materials. There was evidence of abrasive and adhesive wear, which are synonymous with “sliding” conditions along the tooth or chip interface and are indicative of the good machinability of these materials.

- It can be concluded from the work that the fundamental machining characteristics of the workpiece material play a significant role in determining which wear mechanisms are prevalent and should be considered when developing a tool

design/surface coating system for the described machining applications.

## 6. Acknowledgements

The authors wish to express their thanks and appreciation to members of the following organizations for their support:

Materials Research Institute, Sheffield Hallam University,  
Department of Mechanical Engineering, University of Sheffield,

The EPSRC and the Rolling Grant Consortium;  
Universities of Hull and Northumbria at Newcastle,  
James Neill plc, Sheffield,  
Inco Alloys International, Hereford.

## References

1. R. EDWARDS, *Cutting tools*, Institute of Materials, London, (1993), p. 36.
2. A. MATTHEWS, in Proceedings of the Autumn Meeting of the Institute of Metals, 19–21 September 1989, Sheffield, U.K., Institute of Metals, London, (1989) p. 51.
3. S. R. BRADBURY et. al., *Surf. Coat. Tech.* **85** (1996) p. 215.
4. M. SARWAR and P. J. THOMPSON, *Prod. Eng.* **June** (1974) 195.
5. G. BOOTHROYD, "The fundamentals of metal machining" (Edward Arnold, London, 1965) p. 18.
6. M. SARWAR, et al. in Proc. Int. Conf. Adv. Mats and Proc. Tech., Dublin, August 1993, p. 1939.
7. P. W. BREITZIG, "Metals Handbook," Vol. 16, 9th Ed. (ASM International, Metals Park, Ohio, 1989), p. 835.
8. P. K. WRIGHT and E. M. TRENT, *J. Iron and Steel Inst.* **211** (1973) 364.
9. E. M. TRENT, "Metal Cutting" (Butterworths, London, 1977) p. 82.

*Received 18 August 1997  
and accepted 29 July 1998*